

# Band structure and optical absorption of strained $\text{Si}_{1-x-y}\text{Ge}_x\text{C}_y$ alloys: a Tight-Binding approach.

D. Rideau\*, O. Jeannin†, A. Arnaud\*, J. Grebot\*, I. Nicholson†, R. Helleboid\*, G. Mugny†

\* STMicroelectronics, Technology and Design Platforms, France

† STMicroelectronics, Imaging Division, France/United Kingdom

**Abstract**—In this paper, the computation of the band structure and critical energy transition points of ternary random alloys is discussed within the Virtual Crystal Approximation (VCA) in a Tight-Binding (TB) framework. An improved VCA model for  $\text{Si}_{1-x-y}\text{Ge}_x\text{C}_y$  (hereafter referred as SiGeC) is presented, which accurately describes the main energy transitions and shows good agreement with random crystal supercell calculations. Following [1], these transition energies are used to infer the variation of the SiGeC optical absorption in the Near and Short-Wavelength Infrared (resp. NIR and SWIR) as a function of composition and strain. Our model provides a physical-based tool for materials screening for opto-electronics application. Finally the optical parameters are used to simulate and predict the optical absorption of SiGeC resonant cavities.

## I. Introduction

Recently, image sensors working in the NIR/SWIR spectrum have gained interest and are seen as a fast growing area in the future image sensor market [2]. Since Si absorbs weakly or not at all at these wavelengths, a variety of alternative materials are used in industrial development and intensively studied in the literature, such as SiGe, InGaAs alloys, as well as colloidal Quantum Dots [3].

Among them, SiGe alloys can be grown epitaxially on Si CMOS wafers, but defects can occur due to lattice mismatch. To release the strain, smaller C atoms are typically added to form ternary SiGeC alloys, which can be lattice matched with Si wafer [4]. However, the electrical and optical properties of random SiGeC ternary alloys can be greatly influenced by their composition and strain, giving a broad range of parameters.

While the effect of strain and composition on the band structure of SiGe binary alloy has been intensively studied in the literature, using semi-empirical models such as TB or  $k \cdot p$  models carefully fitted on ab initio simulations [5], [6], modelling ternary SiGeC alloys show a higher level of complexity and previous studies have mainly focused on their electronic transport properties [7], [8], [9].

A simulation tool able to predict strained SiGeC optical absorption is thus key for material screening, for the development of devices where optical properties matter.

## II. Methodology

In this paper,  $sp^3d^5s^*$  TB model is used to compute the band structure of SiGeC materials [10], using parameters from [6] for Si and Ge, and newly fitted parameters for C.

### A. Random supercell method

In order to compute the band gap of disordered alloys, Si, Ge and C atoms are placed randomly within a supercell, and their position is relaxed through a valence force field model [11]. The size of the supercell is key and typically needs to be sufficiently large to be representative of a fully disordered system and to avoid supercell-finite-size artefacts. However, the numerical cost of simulation also rapidly increases with supercell size. In this study, we used a supercell of 256 atoms, showing band gap energies in good agreement with experimental data (see Fig. 1) and providing a good trade-off between accuracy and speed.

This method allows to compute the lowest energy transition without further fitting parameters than the ones of pristine Si, Ge and C. However, in the case of a large supercell, the band structure of random alloys is not clearly defined and folds into a very narrow range of  $k$  points. While methods have been proposed to unfold the supercell Brillouin zone [12], the position of main optical gaps, e.g. needed in the model in [1], are difficult to extract accurately.

### B. Virtual Crystal Approximation

Another way to describe random alloys is to build a periodic virtual crystal composed of a single cell with pseudo-atoms whose parameters are interpolated between the pristine atoms, so-called VCA. A linear interpolation is very often not sufficient, and additional ‘bowing’ coefficients need to be fitted to account for the correct band gap variation.

We develop here a new VCA model for SiGeC. Unlike usual VCA models for SiGe, we define here two different atom types in the primitive unit cell, denoted atoms  $A$  and  $B$ . Their on-site parameters are interpolated as follows:

- For  $x < 0.5$  (respectively  $y < 0.5$ ):  $A$ ’s parameters are the ones of pristine Si, and  $B$ ’s parameters are linearly interpolated between Si and Ge (respectively C);
- For  $x > 0.5$  (respectively  $y > 0.5$ ):  $A$ ’s parameters are linearly interpolated between Si and Ge (respectively C);  $B$ ’s parameters are the ones of pristine Ge (respectively pristine C).

The hopping parameters are interpolated as [13]:

$$\begin{aligned}
V_{A,B}^{hop} = & (1-x-y)V_{Si,Si}^{hop} \left( \frac{d_{Si}}{d_{VCA}} \right)^{\eta_{VCA}} \\
& + (x)V_{Ge,Ge}^{hop} \left( \frac{d_{Ge}}{d_{VCA}} \right)^{\eta_{VCA}} \\
& + (y)V_{C,C}^{hop} \left( \frac{d_C}{d_{VCA}} \right)^{\eta_{VCA}} \\
& + P_{A,B}(1-x)x + P_{A,B'}(1-y)y
\end{aligned}$$

where  $\eta_{VCA}$  are the Harrison parameters of VCA crystal linearly interpolated such as:  $\eta_{VCA} = (1-x-y)\eta_{Si} + x\eta_{Ge} + y\eta_C$  and  $d_{VCA}$  is the nearest neighbour distance, interpolated as:  $d_{VCA} = (1-x-y)d_{Si} + xd_{Ge} + yd_C - p_{A,B}(1-x)x + p_{A,B'}(1-y)y$ .  $p_{A,B'}$  and  $p_{A,B}$  coefficients are fitted to reproduce the correct bowing of lattice parameter, and  $P_{A,B}$  and  $P_{A,B'}$  coefficients allow to reproduce the correct band gap variation.

In order to account for epitaxial strain (typically SiGeC grown on Si buffer), the in-plane lattice parameter is fixed to the buffer one and only the atomic position (as well as the outplane lattice parameter) inside the cell are relaxed.

This optimized model's predictions compare favourably with the experimental and random supercell calculations (Fig. 1).

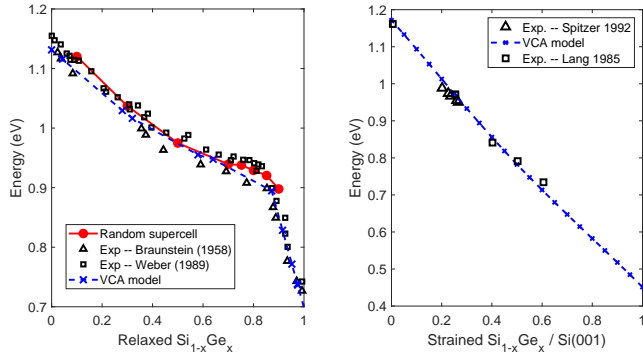


Fig. 1. Band gap of unstrained (left) and strained (right) SiGe alloys as a function of Ge content. Experimental data are from [14]-[15] (left) and [16]-[17] (right). Both random supercell and virtual crystal simulation show good agreement with experimental data.

Extending the work of [1] to strained SiGeC, we use the TB energy transition to define the position of different Dielectric Function Parametric Model oscillators, in order to predict its dielectric constant. As we focus on the IR wavelengths, lowest energy transition near the band gap are mainly studied here.

### III. Results and discussion

#### A. Critical energy points

Fig. 2 shows the position of  $\Delta$  valleys band gaps in SiGeC extracted with VCA model. One can clearly observe the breaking of degeneracy in the  $\Delta$  symmetry point due to strain when Ge and C content is increased. Interestingly,

the effect of C content is different for Si-rich or Ge-rich side of the curve: it lowers the  $\Delta_1$  valley on the Si-rich side of the curve, while the band gap in Ge-rich side is mainly affected by the increase of energy of the  $\Delta_{2,3}$  energy. One also notes that the valence band offset and  $\Delta_2$  valley computed with VCA model are in good agreement with the measurement from [18] and [19]. Similar transition extractions are performed for the main optical transition of [1], in particular for L and  $\Gamma$  valleys.

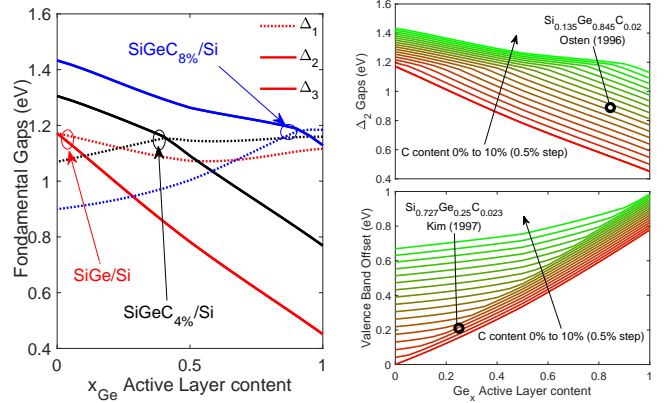


Fig. 2. Left: Position of band gaps at  $\Delta_1$ ,  $\Delta_2$  and  $\Delta_3$  symmetry points in SiGeC strained on Si(001) wafers, computed with TB VCA model. Right:  $\Delta_2$  and valence band offset as a function of Ge content, for different C content. The experimental data from [18] and [19] are also shown in black symbols.

The band structure of SiGe(C) alloys with 40% Ge content obtained with VCA model is also shown in Fig. 3, for 0% and 3.4% C content. One note that the  $\Delta$  valley degeneracy along X and Z direction, lifted due to strain in  $Si_{0.6}Ge_{0.4}$ , is recovered with appropriate C addition.

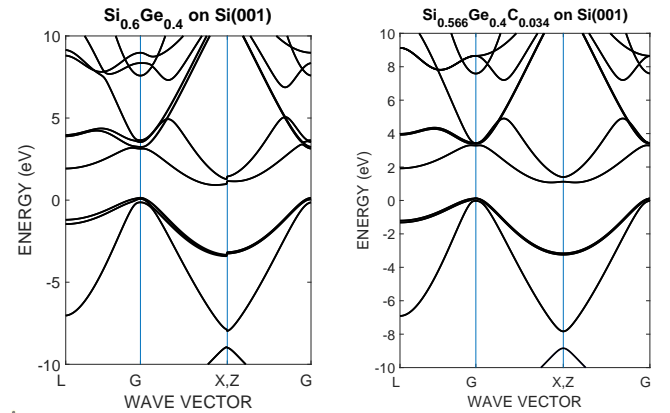


Fig. 3. Band structure of  $Si_{0.6}Ge_{0.4}$  (left) and  $Si_{0.566}Ge_{0.4}C_{0.034}$  (right) strained on (001)Si wafer with VCA model. Adding 3.4% of C allows to relaxed the compressive strain induced by 40% of Ge content in SiGeC alloys.

#### B. Optical absorption

Fig. 4 shows the optical absorption in the NIR (950nm) and SWIR ( $1.3\mu m$ ) wavelengths for strained SiGeC

ternary alloys on (001) Si, as a function of Ge content and for different C content. As expected, Si-rich alloys absorb very poorly in the SWIR and increasing the Ge content in binary SiGe increases strongly the optical absorption in both the NIR and SWIR, by more than two decades, thanks to the reduction of band gap. The situation is more complex for ternary SiGeC alloys: (i) when C is added to pristine Si, the optical absorption is strongly increased, especially in the SWIR wavelengths, as expected from our analysis of  $\Delta_1$  valley in Fig. 2. However, when C is added to pristine Ge, the optical absorption monotonously decreases by more than a decade, in both NIR and SWIR, due to the increase of energy of the  $\Delta_{2,3}$  valleys. One notes again the good agreement between our model and the experimental data from [19].

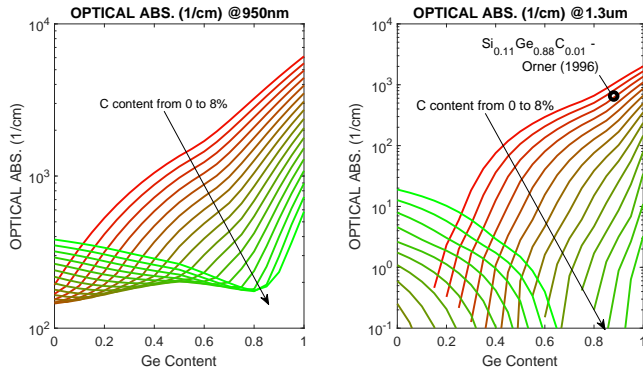


Fig. 4. Optical absorption of strained SiGeC/Si(001) as a function of Ge, for different C contents between 0 and 8% with 0.5% step: for NIR 950nm (left) and SWIR 1.3 $\mu$ m (right) wavelengths. Experimental data from [19] are shown with black circle.

From the variation of lattice parameter, it is possible to extract specific Ge and C concentration that are lattice matched with Si(001) wafer (see Fig. 5). The optical index (n,k) for these specific concentration are plotted in Fig. 5, and show an increase in extinction coefficient when Ge and C content are increased. For the refractive index n, we used a linear dependence over Ge content to reproduce experimental trends in [20]  $n(x) = n_{Si} + 0.31 \cdot x$ .

### C. Resonant cavity

Using the optical indices computed with our model presented above, we investigate here the behaviour of a resonant cavity made by different SiGeC alloys. We simulate with the Transfer Matrix Method (TMM) a resonant cavity about 1 $\mu$ m thick, symmetrically surrounded by two distributed Bragg reflector (DBR) and with air as incident medium. The DBR is composed of successive SiO<sub>2</sub> and Si layers of the type: (SiO<sub>2</sub>/Si)<sup>m</sup>SiO<sub>2</sub>, where m will denote the number of layers of the DBR. The higher is the m, the more reflective is the DBR and the stronger is the cavity. As the refractive index varies with Ge concentration, the thickness of the active layer is also slightly adjusted to obtain the highest absorption at

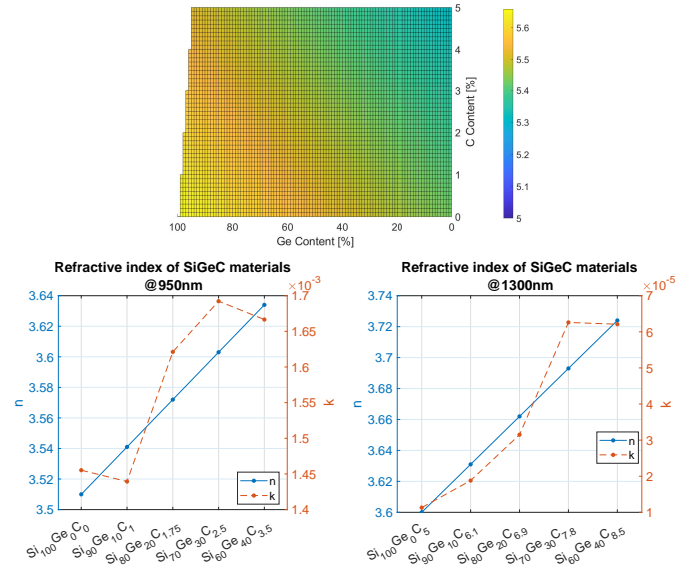


Fig. 5. Top: lattice parameter for SiGeC, as a function of Ge and C content. Bottom: (n,k) optical index at 950nm (left) and 1.3 $\mu$ m (right), for different SiGeC alloys with Ge and C concentration chosen to minimize the stress on Si(001) wafer (lattice matched for 950nm and lattice mismatch less than 2% for 1.3 $\mu$ m).

the desired wavelength. For five-level DBR ( $m = 5$ ), the optical absorption obtained is presented in Fig. 6.

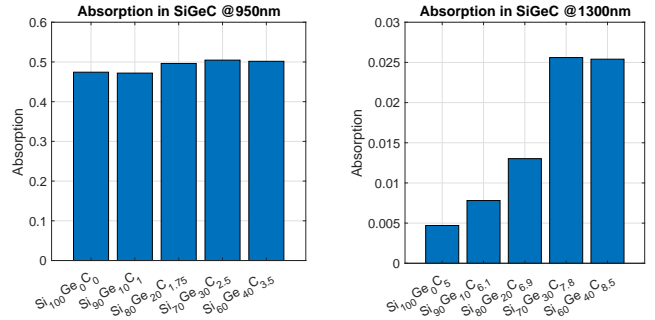


Fig. 6. Optical absorption in the 1 $\mu$ m-thick active layer of a resonant cavity made of two DBR with five-level ( $m = 5$ ) and with active layer made of different SiGeC alloys at 950nm (left) and 1.3 $\mu$ m (right).

One can see that the absorption enhancement by the cavity allows to absorb nearly 50% of the light at 950nm. One also notes that resonant cavity tends to compensate for the extinction coefficient variation: while the extinction coefficient increases by about 18% relative for Si<sub>0.675</sub>Ge<sub>0.3</sub>C<sub>0.025</sub> compared to pure Si, the optical absorption inside the resonant cavity only increases by 10% relative. At 1.3 $\mu$ m wavelength however, the gain in extinction coefficient clearly translates into a gain in optical absorption when Ge and C contents are increased. However, the five-layer DBR resonant cavity doesn't allow to increase optical absorption higher than 2.5%.

In order to boost the optical absorption at 1.3 $\mu$ m, it is possible to improve the cavity gain, by introducing

a higher reflectivity DBR composed of thirteen layers. The thickness of the SiGeC active layer is also decreased around 175nm, which will help growing SiGeC alloys with a slight mismatch on Si(001) wafer, without adding too many defects. As seen in Fig. 7, optical absorption near 50% can also be reached at 1.3 $\mu$ m in this case. One also notes that, in this case, the gain obtained from SiGeC alloys is maintained, and optical absorption is increased from 48% to almost 60% by replacing pure Si by Si<sub>0.79</sub>Ge<sub>0.2</sub>C<sub>0.01</sub> alloy. Let us however note here that this strong cavity with highly reflective mirror also shows a very narrow, monochromatic peak response, which will be very dependant in wavelength and angle of incidence and which is usually not desired in a real application.

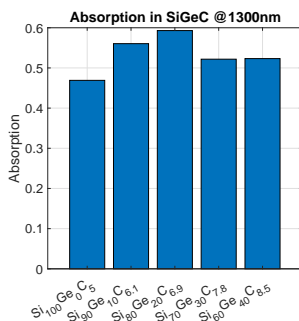


Fig. 7. Optical absorption in the active layer of a resonant cavity at 1.3 $\mu$ m, made of different SiGeC alloys. The thickness of the active layer is here 175nm, which each Bragg mirror are composed of thirteen successive layers of SiO<sub>2</sub> and Si.

#### IV. Conclusion

This paper presents a complete NIR/SWIR optical absorption dataset for strained SiGeC ternary alloys. The versatility of the TB model allows to predict optical absorption near the band edge for any composition, and could be extended to other materials, such as III-V, in further studies. This dataset and model allow to guide materials screening and shows the trade-off between stress relief and optical absorption due to incorporation of C atoms in strained SiGeC on Si wafer. Finally, the optical indices are used in a Transfer Matrix Method tool, to simulate the optical absorption of a resonant cavity.

#### References

- [1] J. Grebot et al., in proceedings of ESSDERC (IEEE), 2021.
- [2] . Yole Développement, "URL: <http://www.yole.fr>."
- [3] D. V. Talapin and J. Steckel, MRS Bulletin, 2013.
- [4] H. J. Osten, Journal of Applied Physics, 1998.
- [5] D. Rideau et al., Physical Review B, 2006.
- [6] Y.-M. Niquet et al., Physical Review B, 2009.
- [7] E. Ramirez-Garcia et al., Solid-state electronics, 2011.
- [8] M. Michailat et al., Thin Solid Films, 2010.
- [9] M. Feraille et al., in 2006 International SISPAD Conference. IEEE, 2006.
- [10] D. Garetto et al., in Proceedings of the 14th International Nanotech Conference, 2011.
- [11] P. Keating, Physical Review, 1966.
- [12] T. B. Boykin et al., Journal of Physics: Condensed Matter, 2007.
- [13] A. Paul et al., Electron Device Letters, IEEE, 2010.

- [14] R. Braunstein et al., Physical Review, 1958.
- [15] J. Weber and M. Alonso, Physical Review B, 1989.
- [16] D. Lang et al., Applied Physics Letters, 1985.
- [17] J. Spitzer et al., Applied physics letters, 1992.
- [18] M. Kim and H. Osten, Applied physics letters, 1997.
- [19] B. Orner et al., Applied physics letters, 1996.
- [20] S. Zollner et al., Journal of Applied Physics, 2000.